MOLECULAR AND CELLULAR BIOLOGY, Nov. 1994, p. 7219–7225
0270-7306/94/$04.00+0

Vol. 14, No. 11

Physical Isolation of Nascent RNA Chains Transcribed by RNA Polymerase II: Evidence for Cotranscriptional Splicing

JÉRÔME WUARIN AND UELI SCHIBLER*

Département de Biologie Moléculaire, Université de Genève, CH-1211 Geneva 4, Switzerland

Received 8 June 1994/Returned for modification 19 July 1994/Accepted 22 August 1994

In order to examine whether splicing can occur cotranscriptionally in mammalian nuclei, we mapped exon-intron boundaries on nascent RNA chains transcribed by RNA polymerase II. A procedure that allows fractionation of nuclei into a chromatin pellet containing DNA, histones, and ternary transcription complexes and a supernatant containing the bulk of the nonhistone proteins and RNAs that are released from their DNA templates was developed. The transcripts of the genes encoding DBP, a transcriptional activator protein, and HMG coenzyme A reductase recovered from the chromatin pellet and the supernatant were analyzed by S1 nuclease mapping. The large majority of the RNA molecules from the pellet appeared to be nascent transcripts, since, in contrast to the transcripts present in the supernatant, they were not cleaved at the polyadenylation site but rather contained heterogeneous 3′ termini encompassing this site. Splicing intermediates could be detected among nascent and released transcripts, suggesting that splicing occurs both cotranscriptionally and posttranscriptionally. Our results also indicate that polyadenylation is not required for the splicing of the last DBP intron. In addition to allowing detailed structural analysis of nascent RNA chains, the physical isolation of nascent transcripts also yields reliable measurements of relative transcription rates.

In higher eukaryotes, the large majority of mRNAs are synthesized as large precursor mRNAs (pre-mRNAs) containing multiple intervening sequences. These sequences are subsequently removed by a process called splicing before the mRNA is transported from the nucleus to the cytoplasm (for reviews see references 11 and 19). As revealed by microscopy studies, actively transcribed genes, polyadenylated RNAs, and components of the splicing machinery appear to colocalize in multiple small subcompartments of the cell nucleus (13, 32). Thus, at least spatially, transcription, polyadenylation, and splicing are closely coupled. The question then arises as to whether splicing can already occur during transcription. In insect cells, this appears to be the case. Evidence for cotranscriptional splicing has been obtained through visualization of transcription complexes by electron microscopy (3, 23) and through kinetic studies of the ecdysone-induced gene *E74A* in *Drosophila melanogaster* (17). Moreover, the analysis of RNA extracted from microdissected Balbiani rings of *Chironomus* larvae revealed the presence of spliced transcripts (2).

Early studies of pre-mRNA processing in mammalian cells have provided evidence for the occurrence of splicing after polyadenylation. This has been suggested by kinetic analysis of globin (1, 8, 14), immunoglobulin (28), and adenovirus mRNA synthesis (20). However, none of these reports could exclude the possibility that introns can also be removed during transcription.

Structural analysis of nascent transcripts would provide the most direct evidence for or against cotranscriptional splicing. In this paper we report the successful physical isolation of nascent pre-mRNA chains from highly purified rat liver cell nuclei. S1 nuclease mapping experiments with albumin site D-binding protein (DBP) and 3-hydroxy-3-methylglutaryl (HMG) coenzyme A (CoA) reductase transcripts present in this nascent RNA fraction and in nuclear RNAs already released from their templates indicate that splicing occurs both cotranscriptionally and posttranscriptionally.

* Corresponding author. Mailing address: Département de Biologie Moléculaire, Sciences II, Université de Genève, 30, Quai Ernest Ansermet, CH-1211 Geneva 4, Switzerland. Phone: 41-22-702 61 75 or 41-22-702 61 97. Fax: 41-22-329 61 02.

MATERIALS AND METHODS

Run-on transcription in isolated nuclei. Liver cell nuclei were isolated from adult male rats (Lewis strain) as described by Lichtsteiner et al. (18) and resuspended in a solution containing 20 mM Tris (pH 7.9), 75 mM NaCl, 0.5 mM EDTA, 0.85 mM dithiothreitol (DTT), 0.125 mM phenylmethylsulfonyl fluoride, 0.1 mg of yeast tRNA per ml, and 50% glycerol, at a concentration of 10^5 nuclei per μl. The elongation of nascent RNA chains was performed as described by Schibler et al. (27), with the following modifications. Nascent RNAs were elongated in the absence of $(NH_4)_2SO_4$ and heparin sulfate. The elongation buffer contained 0.2 μM (instead of 5 μM) [α-^{32}P]UTP (400 Ci/mmol) and 1 mM unlabeled UTP. The elongation was performed for 0, 2, and 5 min at 26°C. The reaction was stopped by the addition of a solution containing 10 volumes of ice-cold 20 mM HEPES (*N*-2-hydroxyethylpiperazine-*N*′-2-ethanesulfonic acid; pH 7.6), 0.2 mM EDTA, 7.5 mM $MgCl_2$, 1 mM DTT, 0.1 mg of yeast tRNA per ml, 0.3 M NaCl, 1% Nonidet P-40, and either 1 M or 2 M urea. The reaction mixture was incubated for 10 min on ice, with occasional agitation, and then centrifuged for 5 min at 4°C in a microcentrifuge.

The chromatin pellet was resuspended in 0.25 ml of a solution containing 10 mM Tris (pH 7.6), 1% sodium dodecyl sulfate (SDS), 20 mM EDTA, and 0.2 mg of proteinase K per ml and incubated at 37°C for 30 min. The mixture was then extracted with phenol-chloroform and precipitated with ethanol. To the chromatin supernatant were added 1% SDS and 0.25 M NaCl, and the solution was phenol-chloroform extracted and ethanol precipitated. After centrifugation, both fractions were washed with 70% ethanol and resuspended in 20 μl of distilled water. A 6-μl portion of each fraction was loaded on a 4% sequencing gel.

Isolation of nascent RNAs. Liver cell nuclei from 32 g of liver tissue were isolated as described by Lichtsteiner et al.

(18), with the addition of 0.1 mg of yeast (*Saccharomyces cerevisiae*) tRNA per ml to both the homogenization buffer and the cushion. Nuclei were then resuspended in 9 ml of a solution containing 20 mM Tris (pH 7.9), 75 mM NaCl, 0.5 mM EDTA, 0.85 mM DTT, 0.125 mM phenylmethylsulfonyl fluoride, 0.1 mg of yeast tRNA per ml, and 50% glycerol and lysed by the addition of 10 volumes of a solution containing 20 mM HEPES (pH 7.6), 1 mM DTT, 7.5 mM $MgCl_2$, 0.2 mM EDTA, 0.1 mg of yeast tRNA per ml, 0.3 M NaCl, 1 M urea, and 1% Nonidet P-40. After vigorous agitation for 5 s, the tubes were left on ice for 10 min. The chromatin was sedimented by centrifugation (15,000 × *g* at 4°C). The supernatant fraction was adjusted to 0.1% with SDS, extracted with phenol-chloroform, and precipitated with ethanol. The chromatin pellet was resuspended in a solution containing 50 mM sodium acetate (NaOAc) (pH 5), 50 mM NaCl, and 0.5% SDS and extracted three times with hot phenol (distilled under nitrogen and containing 0.1 volume of 50 mM NaOAc [pH 5] and 50 mM NaCl) as described by Scherrer (26). Purified RNAs from both the pellet and the supernatant were resuspended in 10 mM Tris (pH 7.5)–0.1% SDS and stored.

Nuclease S1 protection assay. Radiolabeled, single-stranded DNA probes were obtained from genomic DBP subclones as follows. For probe *Bst*EII-*Bgl*II, single-stranded DNA of the DBP coding strand was prepared by coinfection with the helper phage M13KO7 according to the method of Sambrook et al. (25) and used as a template for a primer extension with the oligonucleotide primer 5′-GTAAAACGACGGCCAGT -3′. The primer extension cocktail (30 μl) contained 500 ng of single-stranded template DNA, 50 ng of primer M13-20, 1× Sequenase buffer (U.S. Biochemical [USB] Sequenase kit), 100 mM NaCl, 250 μM (each) deoxynucleoside triphosphates (dNTPs), and 20 U of T7 DNA polymerase (USB). After 10 min at 37°C, DNA was extracted, precipitated, digested with *Bst*EII, extracted with phenol-chloroform, and precipitated. For the labeling reaction at the *Bst*EII site, DNA was resuspended in 20 μl of labeling mix containing 10 mM Tris (pH 7.5); 10 mM $MgCl_2$; 1 mM DTT; 200 μM (each) dGTP, dCTP, and dTTP; 50 μCi of [α-^{32}P]dATP; and 2 U of Klenow enzyme. After 15 min at room temperature, the reaction was stopped by the addition of 40 μl of formamide. The single-stranded, 3′-end-labeled probe was finally isolated by separation on a sequencing gel. The gel band containing the probe was excised, and the DNA was eluted overnight in 0.5 M NH_4OAc–1 mM EDTA. After phenol-chloroform extraction, the DNA was precipitated and resuspended in water. The probe, from 5′ to 3′, comprised 90 nucleotides of KS vector sequence, 100 nucleotides of intron 1, and 386 nucleotides (positions 131 to 517) of exon 1. This probe was labeled at its 3′ end, at the *Bst*EII site located in the first exon of DBP.

The *Bam*HI-*Eco*RV 5′-quasi-end-labeled DBP probe was prepared as follows. The *Bam*HI-*Eco*RV genomic fragment of DBP was cloned into the *Bam*HI-*Eco*RV sites of KS+. This fragment comprised 70 nucleotides of intron 3 and 87 nucleotides of exon 4. Single-stranded DNA containing the coding sequence of DBP was produced with the helper phage K07, as described above. The single-stranded template was annealed with the M13-20 nucleotide primer, and extension was performed in 50 μl of labeling mix containing 500 ng of single-stranded DNA; 50 ng of primer M13-20; 10 mM Tris (pH 7.5); 10 mM $MgCl_2$; 50 mM NaCl; 2 mM DTT; 200 μM (each) dGTP, dCTP, and dTTP; 2 μM dATP; 50 μM [α-^{32}P]dATP; and 2 U of Klenow enzyme. After 10 min at 37°C, 200 μM dATP was added, and the reaction was continued for 10 min at 37°C. The DNA was then extracted, precipitated, and digested with *Hin*dIII, and the single-stranded labeled probe was separated on a sequencing gel and isolated as described above. From the 5′ end to the 3′ end, this probe comprised 90 nucleotides of vector sequence, 87 nucleotides of exon 4, 70 nucleotides of intron 3, and 30 nucleotides of vector sequence.

The single-stranded 3′-end-labeled DBP probe *Nco*I-*Pst*I was prepared by using the following template. The genomic *Eco*RV-*Pst*I fragment was cloned into the vector KS+. This fragment contained the 3′ end of the last exon (positions 1220 to 1667 of the cDNA) as well as 300 nucleotides of the 3′ untranslated region of the DBP gene. Primer extension was initiated from the M13-20 primer, as for the DBP probe described above. After extraction and precipitation, the DNA was digested with *Nco*I (cuts at position 1425 in exon 4) and labeled with Klenow enzyme as described above. The probe comprised, from 5′ to 3′, 90 nucleotides of vector sequence, 300 nucleotides of 3′ untranslated sequences, and 242 nucleotides of exon 4 (positions 1425 to 1667). The probe was 3′ end labeled at the *Nco*I site.

The 5′-quasi-end-labeled HMG CoA reductase probe was prepared as follows. A DNA fragment spanning 100 nucleotides of the first intron and 100 nucleotides of the second exon (obtained by an exonuclease III deletion [30a]) was cloned between the *Apa*I and *Bam*HI sites of the plasmid vector KS+. Primer extension with the oligonucleotide 5′-ACCGTCCCCA CAATAACTTCCCA-3′ and gel purification of the resulting single-stranded fragment were performed as described above for the *Bam*HI-*Eco*RV DBP probe.

For S1 nuclease mapping experiments, DNA probes (50,000 cpm per assay) were coprecipitated with nascent or free nuclear RNAs isolated from 1 g of liver tissue. The pellets were resuspended in 40 μl of 80% formamide–0.4 M NaCl–0.04 M PIPES [piperazine-*N*,*N*′-bis(2-ethanesulfonic acid); pH 6.4]–0.001 M EDTA. The solution was heated for 10 min at 65°C, and hybridization was allowed to occur overnight at 48°C. S1 digestion was carried out as described by Descombes et al. (9).

Western blot (immunoblot) analysis. Liver cell nuclei were lysed and fractionated into a chromatin pellet and a supernatant as described above. The chromatin supernatant was adjusted to 2.5% SDS, 20 mM Tris (pH 6.8), 0.1 M DTT, and 10% glycerol. The chromatin pellet was resuspended in a solution containing 2.5% SDS, 10 mM Tris (pH 6.8), 0.1 M DTT, and 10% glycerol and extensively sonicated, to reduce the viscosity. The proteins from the two fractions were separated by polyacrylamide gel electrophoresis (15) and transferred to a nitrocellulose membrane. Detection of the RNA polymerase II large subunit was performed by using a monoclonal antibody raised against a peptide encompassing three heptapeptide repeats of the C-terminal domain (CTD) (a generous gift of C. Kédinger, Strasbourg, France). The immune complex was visualized with a goat anti-mouse immunoglobulin antibody coupled to horseradish peroxidase by using the Amersham ECL kit.

RESULTS

Separation of nascent RNA from bulk nuclear RNA. In order to examine whether splicing can occur cotranscriptionally, we developed a procedure that allows separation of nuclear RNA into chromatin-associated and released transcripts. The protocol we developed for the fractionation of nuclear RNAs into nascent and released transcripts is based on the extraordinary physical stability of ternary complexes (5). RNA polymerase II, once it has initiated transcription, forms a tight complex with the DNA template that resists treatment with high salt concentrations, polyanions (e.g., heparin sulfate), detergents (e.g., Sarkosyl), and, as shown in this paper,

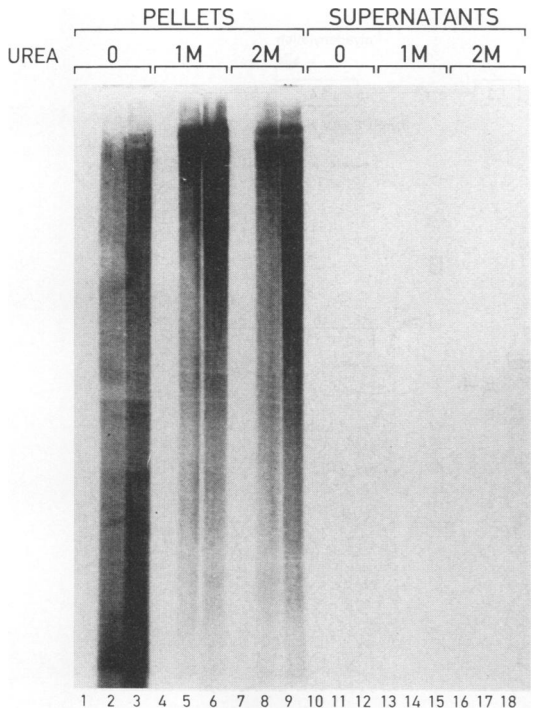

FIG. 1. Ternary transcription complexes are resistant to extraction with NUN buffer. Purified rat liver cell nuclei were incubated for in vitro elongation of nascent transcripts with [α-^{32}P]UTP, lysed with 0, 1, or 2 M urea as indicated (see Materials and Methods), and separated by centrifugation into a chromatin pellet and a supernatant. In vitro-labeled RNAs were extracted from these fractions, displayed on a 4% sequencing gel, and visualized by autoradiography. Incubation times for the labeling of nascent transcripts were 0 min (lanes 1, 4, 7, 10, 13, and 16), 2 min (lanes 2, 5, 8, 11, 14, and 17), and 5 min (lanes 3, 6, 9, 12, 15, and 18).

urea. Extraction of purified nuclei with moderate concentrations of urea in conjunction with the nonionic detergent Nonidet P-40 and 0.3 M NaCl (NUN buffer [16]) provided the most convenient method for the separation of ternary complexes, associated with chromatin, from released RNA. The NUN buffer does not dissociate H1 or core histones from DNA (see below). As a consequence, the chromatin remains highly compacted and can be removed from the nuclear lysate by low-speed centrifugation. In contrast, heparin sulfate- and Sarkosyl-containing buffers, while leaving ternary transcription complexes intact, remove nucleosomes from DNA (10) and thus require high-speed ultracentrifugation for the sedimentation of DNA-associated elongation complexes. This in turn results in the sedimentation of a large amount of released ribonucleoprotein particles and, hence, in a contamination of nascent transcripts with other RNAs (29a).

To examine whether ternary complexes are stable in the NUN extraction buffer, nascent RNA chains present in purified nuclei were pulse-labeled in vitro with [α-^{32}P]UTP before the nuclei were extracted with NUN buffer containing 1 or 2 M urea. RNA was extracted from the supernatant and the chromatin pellet and displayed on a denaturing urea-polyacrylamide gel. As shown in Fig. 1, labeled RNAs were quantitatively retained in the chromatin pellet obtained by a low-speed centrifugation, suggesting that they remained associated with their DNA templates. The average size of in vitro-elongated nascent chains was larger when urea was included in the extraction buffer (Fig. 1; compare lanes 2 and 3 with lanes 5 through 9), suggesting that urea helps to maintain the integrity of RNA during the extraction of nuclei.

If ternary complexes resisted extraction with NUN buffers, RNA polymerases engaged in transcription should be recovered in the chromatin pellet. Figure 2 shows a Western blot analysis with a monoclonal antibody raised against the CTD of the largest RNA polymerase II subunit of proteins recovered from the chromatin pellets and the supernatants. As seen in Fig. 2A, extraction of nuclei with NUN buffers containing 1 or 2 M urea efficiently separated most nonhistone proteins (lanes

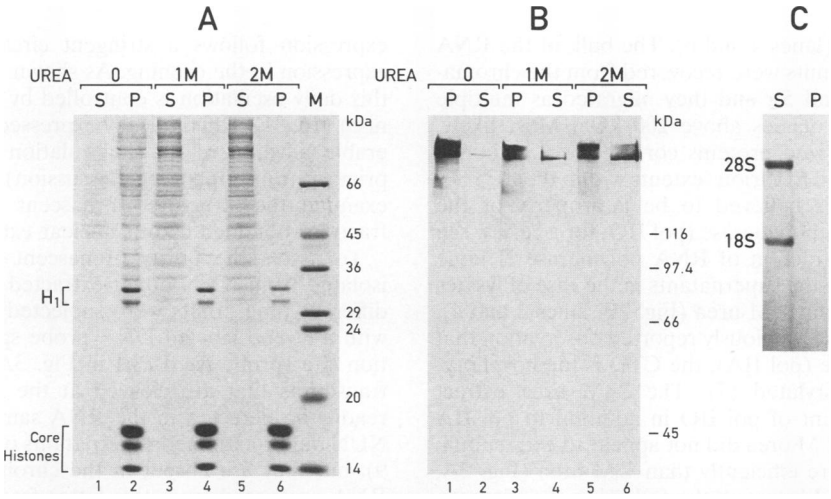

FIG. 2. Analysis of bulk proteins, bulk RNA, and RNA polymerase II in nuclear subfractions. Purified rat liver cell nuclei were incubated with lysis buffers containing 0 to 2 M urea, and the resulting lysates were separated into pellet (P) and supernatant (S) fractions by low-speed centrifugation. Proteins from the pellet and supernatant fractions were analyzed by SDS–12% polyacrylamide gel electrophoresis and Coomassie blue staining (A) or Western blotting (7% polyacrylamide gel) with a monoclonal anti-CTD antibody (B). The positions of H1 histones, core histones, and molecular size markers (M) are indicated. Panel C shows the electrophoretic analysis of RNA, extracted from pellet (P) and supernatant (S) fractions of a NUN buffer-extracted nuclear lysate containing 1 M urea, on a 1.5% agarose gel containing formaldehyde. RNA was visualized by staining with methylene blue after being transferred to a Nytran membrane. The positions of 28S and 18S rRNAs are indicated.

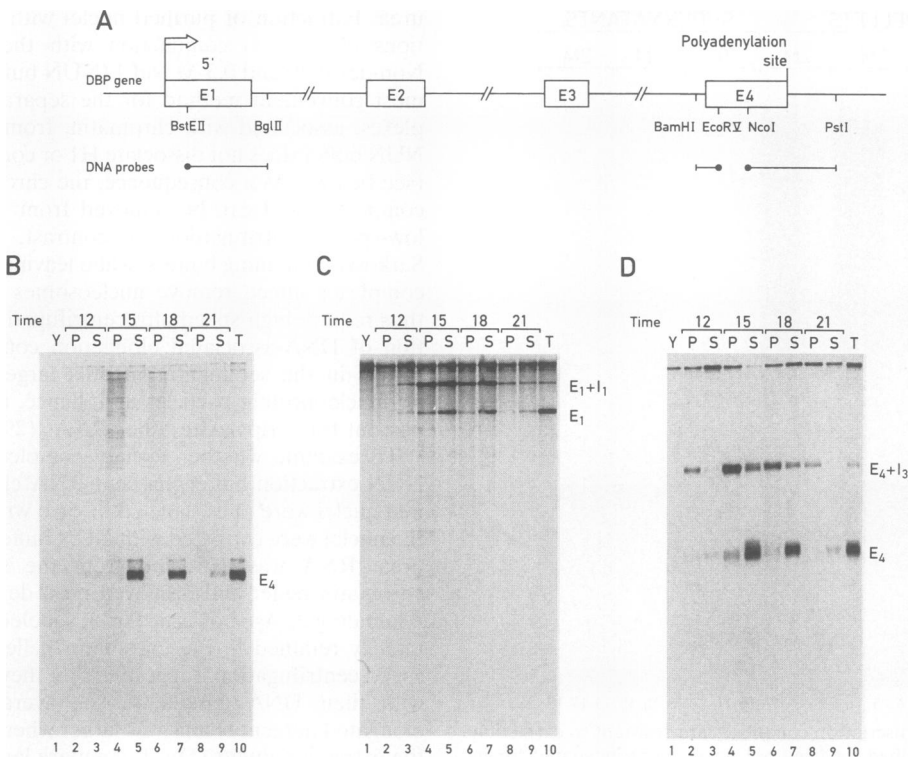

FIG. 3. S1 nuclease mapping of nuclear DBP transcripts. Rat liver cell nuclei, harvested from adult male rats that were sacrificed at four different times of day (indicated above panels B to D), were fractionated into a chromatin pellet (P) and a supernatant (S) after lysis with NUN buffer containing 1 M urea. RNA was extracted from these fractions and characterized by S1 nuclease mapping alongside yeast RNA (Y; negative control) and whole-cell rat liver RNA (T) harvested at 6 p.m. (A) Schematic representation of the exon (E1 to E4)-intron structure of the rat DBP gene. The DBP gene encompasses about 5.6 kb of DNA (9a) from the cap site (arrow) to the polyadenylation site (indicated). The positions of the restriction sites used to prepare the single-stranded DNA probes are indicated. The black dot at the end of each DNA probe indicates the position of the radioactive label. The *Bam*HI-*Eco*RV probe was quasi-end labeled, and it is assumed that most of the radioactive nucleotides were located at positions proximal to the 5′ end of the single-stranded DNA probe. In panels B to D, the positions of S1 nuclease-resistant DNA fragments corresponding to spliced (E) and unspliced (E+I) transcripts are indicated. (B) RNAs mapped with the *Nco*I-*Pst*I DNA probe. The S1 nuclease-resistant exon 4 (E_4) fragment contains about 240 nucleotides. The heterogeneous S1 nuclease-resistant fragments seen in the pellet fractions span up to 540 nucleotides. (C) RNAs mapped with the *Bst*EII-*Bgl*II DNA probe. The sizes of the S1 nuclease-resistant DNA fragments are approximately 490 and 390 nucleotides for E_1+I_1 and E_1, respectively. (D) RNAs mapped with the *Bam*HI-*Eco*RV DNA probe. The sizes of the S1 nuclease-resistant DNA fragments are approximately 160 and 90 nucleotides for E_4+I_3 and E_4, respectively.

3 and 5) from histones (lanes 4 and 6). The bulk of the RNA polymerase II large subunits were recovered from the chromatin pellet (lanes 1, 3, and 5), and they migrated as multiple species with molecular masses above 200 kDa. Most likely, these heterogeneously sized proteins correspond to subunits which are phosphorylated to various extents within their CTDs. CTD phosphorylation is believed to be a property of the elongating form of RNA polymerase (pol IIO; for a review see reference 7). A minor fraction of RNA polymerase II large subunits was observed in the supernatants in the case of lysates that did or did not contain 1 M urea (Fig. 2B, lanes 2 and 4). This is consistent with the previously reported observation that in free RNA polymerase (pol IIA), the CTD is unphosphorylated or underphosphorylated (7). The 2 M urea extract contained a small amount of pol IIO in addition to pol IIA (Fig. 2B, lane 6). Since 2 M urea did not appear to extract bulk nonhistone proteins more efficiently than 1 M urea (Fig. 2A, lanes 4 to 6), we used 1 M urea in the following experiments. This urea concentration was also very efficient in the removal of bulk rRNA from lysed nuclei. As depicted in Fig. 2C, little if any 28S or 18S rRNA remained associated with the NUN buffer-extracted chromatin pellet.

Characterization of nascent DBP and HMG CoA reductase transcripts. DBP is a liver-enriched transcription factor whose expression follows a stringent circadian rhythm with peak expression in the evening. As shown by nuclear run-on assays, this daily oscillation is controlled by a transcriptional mechanism (16, 31). Rhythmically expressed genes may offer considerable advantages for the isolation and characterization of primary transcripts (see Discussion). We therefore chose to examine the structure of nascent DBP transcripts in the fractions obtained by our nuclear extraction procedure.

To assess the purity of nascent DBP transcripts, RNAs isolated from NUN buffer-extracted nuclei harvested at four different time points were subjected to S1 nuclease mapping with a 3′-end-labeled DNA probe spanning the polyadenylation site (probe *Nco*I-*Pst*I in Fig. 3A). As shown in Fig. 3B, transcripts that are cleaved at the polyadenylation site can readily be detected in the RNA samples recovered from the NUN buffer-extracted supernatants of nuclei (lanes 3, 5, 7, and 9), but they are absent in the chromatin pellet. Instead, the RNA recovered from this latter fraction possesses heterogeneous 3′ termini, many of which map to positions downstream of the polyadenylation site (Fig. 2B, lanes 4 and 6). These heterogeneous molecules are resistant to DNase treatment but sensitive to RNase A treatment (data not shown), and their levels follow a circadian rhythm. Thus, they represent bona fide DBP transcripts rather than partially degraded DNA frag-

ments contaminating the RNA preparations. In conclusion, the RNA molecules recovered from the NUN buffer-extracted chromatin pellet appear to consist primarily, if not exclusively, of nascent RNA chains associated with elongating transcription complexes.

Having established the validity of our fractionation procedure, we wished to examine whether the nascent RNA chains contained already spliced molecules. To this end the NUN buffer-fractionated RNAs were mapped with two DNA probes, *Bst*EII-*Bgl*II and *Bam*HI-*Eco*RV, which spanned the splice donor site of the first intron and the splice acceptor site of the third intron, respectively (Fig. 3A). The results obtained in these S1 mapping experiments are presented in Fig. 3C and D. As expected, the DBP transcripts recovered from the NUN buffer-extracted supernatant were composed of RNAs that spanned the entire DBP sequence contained in the DNA probes (labeled as E_1+I_1 and E_4+I_3 in Fig. 3C and D, respectively) and RNAs that had already undergone splicing at the examined junctions (labeled as E_1 and E_4 in Fig. 3C and D, respectively). Significantly, these same RNA species could also be observed in the NUN buffer-extracted pellet containing the nascent transcripts. This suggests that a fraction of template-associated transcripts had undergone splicing at these junctions. While DBP transcripts spliced at either of the two examined exon/intron junctions could be discerned in both released and chromatin-associated RNA, their relative contributions to these fractions differed. DBP transcripts not yet spliced at the exon 1/intron 1 (E1/I1) junction dominated over the spliced form in both chromatin-associated and released RNA (e.g., that in Fig. 3C, lanes 4 and 5). This is in contrast to the results obtained with molecules spliced at the E4/I3 junction. Here, nonspliced transcripts were more abundant only in the chromatin in putative nascent RNAs (e.g., those in Fig. 3D, lane 4). In released RNA (e.g., that in Fig. 3D, lane 5), most (but not all) transcripts were already processed at the E4/I3 junction. A possible interpretation of these results is presented in Discussion.

HMG CoA reductase is the rate-limiting enzyme in the pathway of cholesterol synthesis (4). The accumulation of the mRNA encoding this protein, like that of DBP mRNA, also oscillates during the day (6). However, peak levels of HMG CoA reductase mRNA are observed between 10 p.m. and 12 midnight, several hours later than the time at which maximal DBP mRNA concentrations are reached (29a). To examine whether nascent HMG CoA reductase transcripts are also spliced cotranscriptionally, an S1 nuclease mapping experiment, similar to the one described for DBP in the legend to Fig. 3, was performed. A 5′-end-labeled restriction fragment encompassing the splice acceptor site of the first intron was used as a probe (see Materials and Methods). As shown in Fig. 4B (lane 10), S1 nuclease mapping of whole-cell RNA produced two major protected bands, E_2 and E_2+I_1, corresponding to spliced and unspliced HMG CoA reductase transcripts, respectively. Both of these transcripts were also observed with the RNAs extracted from the fractions containing nascent (Fig. 4, lanes 4, 6, and 8) and released (lanes 3, 5, 7, and 9) nuclear RNAs. Thus, in a manner similar to that for nascent DBP RNAs, a significant proportion of HMG CoA reductase transcripts appeared to undergo cotranscriptional processing.

Some bands between the ones corresponding to the E_2+I_1 and E_2 transcripts can also be discerned. The relative intensities of these minor bands are about equal to that of the same fraction of the E_2+I_1 band in RNA directly extracted with guanidium thiocyanate from fresh liver tissue and that of RNA isolated from subnuclear fractions (compare lanes 4 and 9 of Fig. 4). Therefore, these minor bands do not appear to result from RNA degradation during subcellular fractionation, but rather they reflect the presence of S1 nuclease-hypersensitive sites within E_2+I_1 RNA-DNA hybrids.

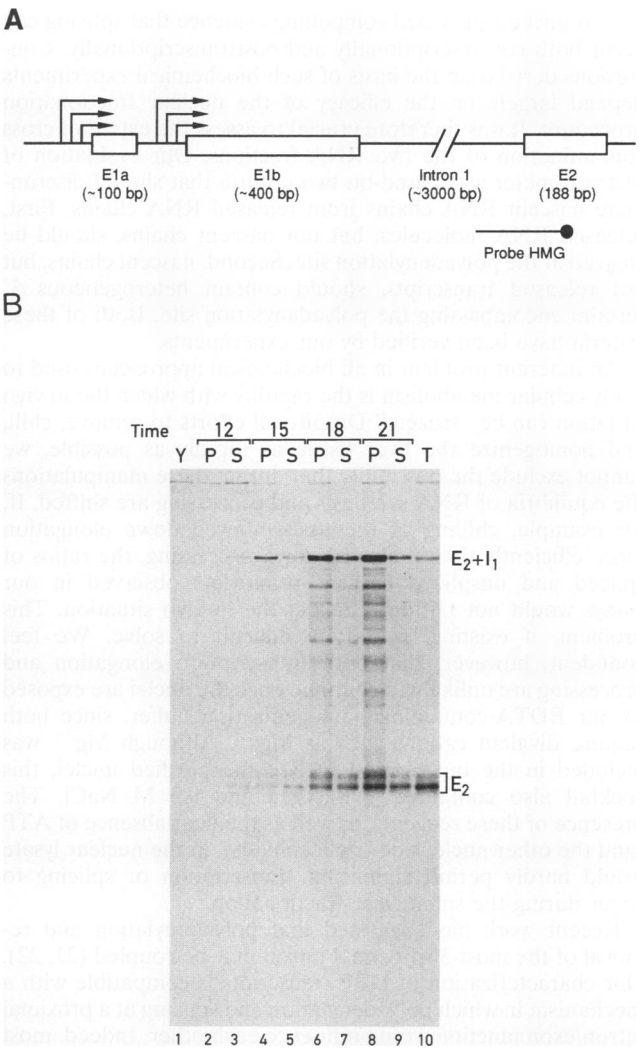

FIG. 4. S1 nuclease mapping of nuclear HMG CoA reductase transcripts. (A) Schematic map of the 5′ moiety of the rat HMG CoA reductase gene (31a). This gene contains two promoters, each containing multiple start sites (indicated by three arrows for each promoter) and two alternative first exons. A quasi-end-labeled primer, encompassing about 100 nucleotides each of intron 1 and exon 2 (E2), was used for the S1 nuclease mapping experiment (indicated below the gene map; the filled circle indicates that the probe was quasi-end labeled at the 5′ end). (B) The subnuclear RNA fractions described in the legend to Fig. 3 were analyzed by S1 nuclease mapping with the 5′ quasi-end-labeled DNA probe described above. The positions of S1 nuclease-resistant DNA fragments corresponding to spliced (E_2; 96 nucleotides) and unspliced (E_2+I_1; approximately 200 nucleotides) transcripts are indicated. Yeast RNA (Y; negative control) and whole-cell RNA (T; positive control) were included in the S1 nuclease mapping experiments. Analyses were performed at the indicated times of day.

DISCUSSION

Here we report the successful fractionation of nuclear RNA into nascent transcripts and RNAs that are released from their DNA templates. S1 mapping of these RNAs with end-labeled DNA probes specific for the genes encoding DBP and HMG

CoA reductase provided compelling evidence that splicing can occur both cotranscriptionally and posttranscriptionally. Conclusions derived on the basis of such biochemical experiments depend largely on the efficacy of the nuclear fractionation procedure. It was therefore crucial to assess the extent of cross contamination of the two RNA fractions. Our evaluation of this parameter was based on two criteria that should discriminate nascent RNA chains from released RNA chains. First, released RNA molecules, but not nascent chains, should be cleaved at the polyadenylation site. Second, nascent chains, but not released transcripts, should contain heterogeneous 3′ termini encompassing the polyadenylation site. Both of these criteria have been verified by our experiments.

An inherent problem in all biochemical approaches used to study cellular metabolism is the rapidity with which the in vivo situation can be "frozen." Despite all efforts to remove, chill, and homogenize the liver tissue as rapidly as possible, we cannot exclude the possibility that during these manipulations the equilibria of RNA synthesis and processing are shifted. If, for example, chilling of the tissue slowed down elongation more efficiently than it slowed down processing, the ratios of spliced and unspliced nascent transcripts observed in our assays would not faithfully reflect the in vivo situation. This problem, if existing, would be difficult to solve. We feel confident, however, that both transcription elongation and processing are unlikely to continue once the nuclei are exposed to our EDTA-containing homogenization buffer, since both require divalent cations such as Mg^{2+}. Although Mg^{2+} was included in the buffer used to lyse the purified nuclei, this cocktail also contained 1 M urea and 0.3 M NaCl. The presence of these reagents, as well as the near absence of ATP (and the other nucleoside triphosphates), in the nuclear lysate would hardly permit significant transcription or splicing to occur during the subnuclear fractionation.

Recent work has suggested that polyadenylation and removal of the most 3′-proximal intron may be coupled (21, 22). Our characterization of DBP transcripts is compatible with a mechanism in which polyadenylation and splicing at a proximal intron/exon junction would influence each other. Indeed, most of the released nuclear DBP transcripts were both polyadenylated and spliced at the last intron/exon junction (Fig. 3B and D, lanes 5 and 7). Yet a minor (but clearly detectable) fraction of nascent DBP transcripts appeared to be spliced at this exon/intron boundary (e.g., those in Fig. 3D, lanes 4 and 6). Thus, while polyadenylation may increase the rate of last intron removal, it is unlikely to be an obligatory requirement for such removal. A similar conclusion was reached by Baurén and Wieslander (2) in the study of Balbiani ring transcripts.

Evidence for cotranscriptional splicing has already been reported for *Drosophila* and *Chironomus* genes (2, 3, 17, 23). The elegant work of Baurén and Wieslander (2) demonstrates that, in the case of Balbiani ring 1 transcripts, the extent of cotranscriptional splicing depends on kinetic parameters, such as the RNA polymerase II elongation rate and the rates at which spliceosomes are assembled and introns are removed. Therefore, 5′-proximal Balbiani ring 1 introns undergo more extensive cotranscriptional splicing than 3′-proximal ones. Somewhat unexpectedly, we did not observe dramatic differences between cotranscriptional splicing of the first DBP intron and that of the last DBP intron (compare the ratios of E_1+I_1 to E_1 and E_4+I_3 to E_4 in pellet fractions of Fig. 3C and D). This may suggest that RNA polymerase II elongation complexes stall for a relatively long time at sites located downstream of the DBP polyadenylation site. The size distribution of the nascent DBP transcripts revealed in Fig. 3B (lanes 4 and 6) would be consistent with this speculation. Indeed, transcripts mapping to nucleotide positions downstream of the polyadenylation site appear to be more abundant than the ones mapping to positions located upstream of this site. It is feasible that a clear polarity of cotranscriptional splicing can only be observed with relatively large genes, such as those specifying Balbiani ring 1 (40 kb) or *E74A* (60 kb) transcripts mentioned above. From the comparison of Fig. 3C and 4B, it appears that cotranscriptional splicing of 5′-proximal introns is somewhat more extensive for HMG CoA reductase transcripts than for DBP transcripts. This would be consistent with the much larger size of the former gene compared with the latter gene. In hamsters, the HMG CoA reductase gene is composed of 20 exons and encompasses more than 25 kb (24). Unfortunately, recombinant DNAs encompassing the 3′-proximal moiety of the rat HMG CoA reductase gene are not yet available. We were thus unable to examine the polarity of cotranscriptional splicing in this case.

At constant transcription and degradation rates, the steady-state mRNA-to-pre-mRNA ratio is roughly the ratio obtained by dividing the mRNA half-life by the time required to convert 50% of the pre-mRNA into cytoplasmic mRNA molecules (note that the synthesis and nuclear stability of pre-mRNA affect the absolute levels of pre-mRNA and mRNA but not the ratio between the two). For very stable mRNAs this ratio is very high and may thus complicate the analysis of nascent transcripts, since even a small contamination of nuclei with cytoplasm could result in a relatively large contamination of pre-mRNA with mature mRNA. Anticipating such problems, we selected DBP and HMG CoA reductase transcripts for our initial analysis. The synthesis and accumulation of both of these mRNAs follow a daily rhythm with a strong amplitude (6, 31). This increases the pre-mRNA/mRNA ratio in two ways. First, in order to cycle during the day, the mature mRNAs must necessarily be short-lived (for a mathematical model, see reference 30); second, at the time of maximal pre-mRNA synthesis, maximal mRNA levels have not yet been reached. Our S1 nuclease mapping experiments confirmed both of these predictions. Even whole-cell RNA contains a readily detectable proportion of unspliced DBP and HMG CoA reductase mRNA (Fig. 3B through D and 4B, lanes 10), reflecting the short half-lives of DBP and HMG CoA reductase mRNAs. Furthermore, maximal transcription rates, as estimated by the relative amounts of nascent DBP and HMG CoA transcripts (Fig. 3 and 4), are reached at 3 and 9 p.m., respectively, thus preceding the time of maximal mRNA accumulation (6, 29a, 31). In the case of the DBP gene, circadian transcription has also been evaluated by nuclear run-on experiments (16). The results are entirely consistent with those produced by the quantitation of physically isolated nascent chains by S1 nuclease mapping, further establishing the validity of this latter method.

We wish to reemphasize that the successful isolation of nascent chains, which represent only a minute fraction of cellular RNA, requires an efficient procedure for the purification of nuclei. Particularly problematic would be the contamination of nuclei with unbroken cells, in which cytoplasm contributes the bulk of cellular RNA. Phase-contrast-microscopical examination of rat (or mouse) liver cell nuclei sedimented through 2 M sucrose revealed a complete absence of unbroken cells (data not shown). The purity of the liver cell nuclei was further examined biochemically by estimating the relative amounts of the cytoplasmic enzyme glutathione *S*-transferase in a liver homogenate and in purified nuclei. This enzyme accumulates to very high concentrations in parenchymal hepatocytes. Coomassie blue staining of electrophoretically separated, affinity-purified glutathione *S*-transferase (29)

revealed that the nuclei contained less than 1/1,000 of the enzyme originally present in the liver lysate (18a).

As pointed out above, our nascent chain mapping experiments have thus far been restricted to short-lived transcripts. However, given the nearly complete extraction of bulk RNA from the chromatin pellet (Fig. 3C), we expect that this procedure will be applicable for the isolation of nascent pre-mRNA from most genes, provided that highly purified nuclei can be obtained from the cells under study. The physical isolation and characterization of nascent RNA chains may thus offer an alternative, perhaps more versatile approach to nuclear run-on transcription in isolated nuclei (10, 12) for the estimation of relative transcription rates. In particular, for gene families composed of several closely related members, the RNA synthesis rates cannot be assessed accurately for an individual family member by run-on transcription assays. In vitro-elongated nascent RNA chains of all highly similar genes would cross-hybridize in such experiments with the filter-bound DNA probes. In contrast, even small sequence differences between nascent transcripts of similar, but not identical, genes can readily be discerned by S1 nuclease or RNase mapping of nascent transcripts. Thus, the specificity, sensitivity, and ease of manipulation of the mapping of nascent RNAs may render this procedure widely applicable in the study of transcriptional and posttranscriptional control mechanisms in eukaryotic cells.

ACKNOWLEDGMENTS

We are grateful to Claude Kédinger for his generous gift of a monoclonal CTD antibody and to Daniel Lavery for his valuable advice on the NUN buffer extraction procedure. The critical and helpful comments of Edward Schmidt and Daniel Lavery greatly improved the manuscript.

This work was supported by the Swiss National Science Foundation, the Canton of Geneva, and the Roche Research Foundation.

REFERENCES

1. **Bastos, R. N., and H. Aviv.** 1977. Globin RNA precursor molecules: biosynthesis and processing in erythroid cells. Cell **11**:641–650.
2. **Baurén, G., and L. Wieslander.** 1994. Splicing of Balbiani Ring 1 gene pre-mRNA occurs simultaneously with splicing. Cell **76**:183–192.
3. **Beyer, A. L., and Y. N. Osheim.** 1988. Splice site selection, rate of splicing, and alternative splicing on nascent transcripts. Genes Dev. **2**:754–765.
4. **Brown, M. S., and J. L. Goldstein.** 1980. Multivalent feedback regulation of HMG CoA reductase, a control mechanism coordinating isoprenoid synthesis and cell growth. J. Lipid Res. **21**:505–517.
5. **Cai, H., and D. S. Luse.** 1987. Transcription initiation by RNA polymerase II *in vitro*. J. Biol. Chem. **262**:298–304.
6. **Clarke, C. F., A. M. Fogelman, and P. A. Edwards.** 1984. Diurnal rhythm of rat liver mRNAs encoding 3-hydroxy-3-methylglutaryl coenzyme A reductase. J. Biol. Chem. **259**:10439–10447.
7. **Corden, J. L.** 1993. RNA polymerase II transcription cycles. Curr. Opin. Genet. Dev. **3**:213–218.
8. **Curtis, P. J., N. Mantei, J. Van den Berg, and C. Weissmann.** 1977. Presence of a putative 15S precursor to β-globin mRNA but not to α-globin mRNA in Friend cells. Proc. Natl. Acad. Sci. USA **74**:3184–3188.
9. **Descombes, P., M. Chojkier, S. Lichtsteiner, E. Falvey, and U. Schibler.** 1990. LAP, a novel member of the C/EBP family, encodes a liver-enriched transcriptional activator protein. Genes Dev. **4**:1541–1551.

9a. **Falvey, E., and U. Schibler.** Unpublished data.

10. **Gariglio, P., M. Bellard, and P. Chambon.** 1981. Clustering of RNA polymerase B molecules in the 5′ moiety of the adult β-globin gene of hen erythrocytes. Nucleic Acids Res. **9**:2589–2598.
11. **Green, M. R.** 1991. Biochemical mechanisms of constitutive and regulated pre-mRNA splicing. Annu. Rev. Cell Biol. **7**:559–599.
12. **Groudine, M., M. Peretz, and H. Weintraub.** 1981. Transcriptional regulation of hemoglobin switching in chicken embryos. Mol. Cell. Biol. **1**:281–288.
13. **Jiménez-Garcia, L. F., and D. L. Spector.** 1993. *In vivo* evidence that transcription and splicing are coordinated by a recruiting mechanism. Cell **73**:47–59.
14. **Kinniburgh, A. J., J. E. Mertz, and J. Ross.** 1978. The precursor of mouse β-globin mRNA contains two intervening RNA sequences. Cell **14**:681–693.
15. **Laemmli, U. K.** 1970. Cleavage of structural proteins during the assembly of the head of bacteriophage T4. Nature (London) **227**:680–685.
16. **Lavery, D. J., and U. Schibler.** 1993. Circadian transcription of the cholesterol 7α hydroxylase gene may involve the liver-enriched transcription factor DBP. Genes Dev. **7**:1873–1884.
17. **LeMaire, M. F., and C. S. Thummel.** 1990. Splicing precedes polyadenylation during *Drosophila E74A* transcription. Mol. Cell. Biol. **10**:6059–6063.
18. **Lichtsteiner, S., J. Wuarin, and U. Schibler.** 1987. The interplay of DNA-binding proteins on the promoter of the mouse albumin gene. Cell **51**:963–973.

18a. **Marcacci, L., and U. Schibler.** Unpublished data.

19. **Moore, M. J., C. C. Query, and P. A. Sharp.** 1993. Splicing of precursors to mRNAs by the spliceosome, p. 303–357. *In* R. F. Gesteland and J. F. Atkins (ed.), The RNA world. Cold Spring Harbor Laboratory Press, Cold Spring Harbor, N.Y.
20. **Nevins, J. R., and J. E. Darnell, Jr.** 1978. Steps in the processing of Ad2 mRNA: poly(A)+ nuclear sequences are conserved and poly(A)+ addition precedes splicing. Cell **15**:1477–1493.
21. **Niwa, M., and S. M. Berget.** 1991. Mutation of the AAUAAA polyadenylation signal depresses *in vitro* splicing of proximal but not distal introns. Genes Dev. **5**:2086–2095.
22. **Niwa, M., S. D. Rose, and S. M. Berget.** 1992. *In vitro* polyadenylation is stimulated by the presence of upstream introns. Genes Dev. **4**:1552–1559.
23. **Osheim, Y. N., O. L. Miller, and A. L. Beyer.** 1985. RNP particles at splice junction sequences on Drosophila chorion transcripts. Cell **43**:143–144.
24. **Reynolds, G. A., S. K. Basu, T. F. Osborne, D. J. Chin, G. Gil, M. S. Brown, J. L. Goldstein, and K. L. Luskey.** 1984. HMG CoA reductase, a negatively regulated gene with unusual promoter and 5′ untranslated regions. Cell **38**:275–286.
25. **Sambrook, J., E. F. Fritsch, and T. Maniatis.** 1989. Molecular cloning: a laboratory manual, 2nd ed. Cold Spring Harbor Laboratory Press, Cold Spring Harbor, N.Y.
26. **Scherrer, K.** 1969. Isolation and sucrose gradient analysis of RNA, p. 413–432. *In* K. Habel and N. P. Salzman (ed.), Fundamental techniques in virology. Academic Press, New York.
27. **Schibler, U., O. Hagenbüchle, P. K. Wellauer, and A. C. Pittet.** 1983. Two promoters of different strength control the transcription of the mouse alpha-amylase gene Amy-1a in the parotid gland and the liver. Cell **33**:501–508.
28. **Schibler, U., K. B. Marcu, and R. P. Perry.** 1978. The synthesis and processing of the mRNAs specifying heavy and light chain immunoglobulins in MPC-11 cells. Cell **15**:1495–1509.
29. **Smith, D. B., and K. S. Johnson.** 1988. Single-step purification of polypeptides expressed in E. coli as fusions with glutathione-S-transferase. Gene **67**:31–40.

29a. **Wuarin, J.** Unpublished observations.

30. **Wuarin, J., E. Falvey, D. Lavery, D. Talbot, E. Schmidt, P. Ossipow, P. Fonjallaz, and U. Schibler.** 1992. The role of the transcriptional activator protein in circadian liver gene expression. J. Cell. Physiol. **16**(Suppl.):123–127.

30a. **Wuarin, J., D. Lavery, and U. Schibler.** Unpublished results.

31. **Wuarin, J., and U. Schibler.** 1990. Expression of the liver-enriched transcriptional activator protein DBP follows a stringent circadian rhythm. Cell **63**:1257–1266.

31a. **Wuarin, J., and U. Schibler.** Unpublished data.

32. **Xing, Y., C. V. Johnson, P. R. Dobner, and J. B. Lawrence.** 1993. Higher level organization of nuclear structure and function. Science **259**:1326–1330.